AD-E401 160

TECHNICAL REPORT ARLCD-TR-84003

CARS SPECTRA FROM A 7.62-MM GUN

EDWARD D. PETROW
GEO-CENTERS, INC.
NEWTON UPPER FALLS, MA 02164

LEE E. HARRIS
ARDC

MARCH 1984

U.S. ARMY ARMAMENT RESEARCH AND DEVELOPMENT CENTER
LARGE CALIBER WEAPON SYSTEMS LABORATORY
DOVER, NEW JERSEY

APPROVED FOR PUBLIC RELEASE; DISTRIBUTION UNLIMITED.

UNCLASSIFIED

SECURITY CLASSIFICATION OF THIS PAGE (When Date Entered)

REPORT DOCUMENTATION PAGE

READ INSTRUCTIONS BEFORE COMPLETING FORM

1. REPORT NUMBER
Technical Report ARLCD-TR-84003

2. GOVT ACCESSION NO.

3. RECIPIENT'S CATALOG NUMBER

4. TITLE (and Subtitle)
CARS SPECTRA FROM A 7.62-mm GUN

5. TYPE OF REPORT & PERIOD COVERED

6. PERFORMING ORG. REPORT NUMBER

7. AUTHOR(s)
Edward D. Petrow, Geo-Centers, Inc.
Lee E. Harris, ARDC

8. CONTRACT OR GRANT NUMBER(s)

9. PERFORMING ORGANIZATION NAME AND ADDRESS
Geo-Centers, Inc.
Newton Upper Falls, MA 02164
(cont)

10. PROGRAM ELEMENT, PROJECT, TASK AREA & WORK UNIT NUMBERS

11. CONTROLLING OFFICE NAME AND ADDRESS
ARDC, TSD
STINFO Div [DRSMC-TSS(D)]
Dover, NJ 07801

12. REPORT DATE
March 1984

13. NUMBER OF PAGES
39

14. MONITORING AGENCY NAME & ADDRESS(if different from Controlling Office)

15. SECURITY CLASS. (of this report)
Unclassified

15a. DECLASSIFICATION/DOWNGRADING SCHEDULE

16. DISTRIBUTION STATEMENT (of this Report)
Approved for public release; distribution unlimited.

17. DISTRIBUTION STATEMENT (of the abstract entered in Block 20, if different from Report)

18. SUPPLEMENTARY NOTES
The contribution of Geo-Centers, Inc., to this project was accomplished under Contract DAAK10-81-C-0266.

19. KEY WORDS (Continue on reverse side if necessary and identify by block number)
CARS
Raman
Gun flash
Propellants
Combustion

20. ABSTRACT (Continue on reverse side if necessary and identify by block number)
Colinear Coherent Anti-Stokes Raman Scattering (CARS) spectra were obtained from a 7.62-mm MANN gun system. These preliminary experiments, designed to demonstrate the technical feasibility of CARS thermometry for this application, have been successful within the limited scope of the completed experiments. The numerous technical problems encountered are addressed and details of the experimental apparatus are documented. The successful completion of these preliminary experiments clearly demonstrates that CARS thermometry can be a useful analytical
(cont)

9. PERFORMING ORGANIZATION NAME AND ADDRESS (cont)

ARDC, LCWSL
Applied Sciences Div [DRSMC-LCA-G(D)]
Dover, NJ 07801

20. ABSTRACT (cont)

technique for gun and charge designers provided that certain limitations and the level of experimental complexity are acknowledged.

ACKNOWLEDGMENTS

The many helpful discussions and suggestions regarding CARS theory and practice provided by Dr. Kenneth Aron is greatly appreciated. The practical advice concerning the operational details of the gun and instrumentation was generously provided by John Riedener and Lou Behling. Special thanks to Tom Johnson who provided significant technical support and innovation during the experimental portion of the program.

CONTENTS

FIGURES

INTRODUCTION

A detailed knowledge of the thermodynamics and gas dynamics of propellant gases both before and after departing from the gun barrel is required before the numerous problems associated with high performance cannons and projectiles can be solved. Among these problems are:

1. Muzzle flash which, although common to all guns, is of particular significance in artillery weapons

2. Barrel erosion in tank guns caused by high performance ammunition

3. Muzzle blast which can be detrimental to howitzers and large caliber cannons

The specific motivation for this program was muzzle flash. Propellant gases emerging from a gun muzzle interact with the surrounding atmosphere and produce an intense light emission. Earlier detailed investigations of muzzle flash (refs 1 through 7) revealed three distinct luminous regions separated in both space and time: primary (R1), intermediate (R2), and secondary (R3). Although the exact mechanisms associated with the individual flash events are not completely understood, it is generally assumed that R1 is comprised of the hot, highly compressed gas column driven from the gun tube. As these high pressure gases expand adiabatically, due to the large pressure gradient between the two flow fields, they are cooled and their luminosity disappears. Overexpanded gases are then recompressed and heated by passage through a shock front. They are comprised of considerable combustible constituents but little oxygen; however, they can be reignited if their temperature is raised high enough. If this occurs, the subsequent luminosity is termed R2. When combustion at this stage is incomplete because of insufficient oxygen, the blast field may continue to develop and, as ambient air is entrained, another combustion zone is formed which results in R3. Enough combustible material remains at this point that the R3 event has been reported to release as much energy as the initial in-bore combustion (ref 8).

These ignition and combustion events are not well understood and little experimental data is available to support even limited phenomenological modeling efforts (ref 3). Traditionally, evaluation of specific gas properties is made indirectly and is generally limited to the direct measurement of internal pressure and temperature on the gun barrel surface. The flow-field gas temperature and other thermodynamic properties are then inferred from these simple surface measurements with the aid of certain interior ballistics assumptions. Because of the inherent limitations of this approach, the detailed information required for accurate modeling of propellant behavior both in and out of the gun barrel is not available. Optical techniques such as high speed, schlieren, and shadow-graphic photography (ref 5) are useful in flow visualization but are intrinsically incapable of providing quantitative data. More sophisticated optical techniques, such as emission and absorption spectroscopy and multicolor pyrometry, are capable of providing quantitative data but these are integrated over the entire sample region.

Several nonintrusive, high spatial resolution techniques for probing molecular species present in the high temperature flow field at the muzzle of a gun are available to charge and ballistic designers. Although potassium and sodium resonance lines (ref 3), fluorescence and spontaneous Raman (ref 9), and other optical techniques have been employed with varying degrees of success, each has certain limitations and problems and may not offer the designer a simple, informative, and reliable measurement of simultaneous temperature and concentration.

Coherent Anti-Stokes Raman Scattering (CARS) spectroscopy has become one of the leading nonlinear spectroscopic techniques for nonintrusive molecular probing in hostile environments (refs 10, 14, and 15). The technique is particularly well suited for probing of transient, turbulent, incandescent, and particle-laden combustion environments such as propellant flames (ref 11), internal combustion engines (ref 12), and jet engine afterburners (refs 10 and 13). The main advantage of CARS over other popular spectroscopic diagnostics is signal generation efficiency (ref 13). With CARS, this efficiency is several orders-of-magnitude greater than spontaneous Raman, and the coherent signal is collimated, whereas other techniques produce signal photons over 4 π steradians. In addition to these general advantages, the CARS technique offers several others: capability for high spatial resolution (1 mm or better), good accuracy (1% routinely achieved with N_2 CARS thermometry), rapid data acquisition and processing (tens of seconds), and high temporal resolution (10^{-8} seconds) for single pulse experiments. In most classical CARS experiments, evaluations of the post-flame zone composition and characteristics are determined by measuring the temperature and the concentration of major equilibrium products (i.e., N_2, CO, CO_2, H_2, and H_2O). Classical spatial mapping of these flame systems is accomplished using the CARS technique (ref 16), but the same technique can be applied as a tool for evaluating combustion mechanisms or reaction pathways (ref 17).

BACKGROUND

The theory of CARS and its practical experimental applications have been extensively reviewed (ref 16). Briefly, the basis of CARS is the nonlinear response through the third order susceptibility of a homogeneous medium upon which waves of the pump laser beam (ω_1) and the Stokes laser beam (ω_2) are incident. Vibrational resonant enhancement (CARS signal) is observed if the difference between the frequencies of ω_1 and ω_2 are equivalent to a real Raman-active vibrational frequency of a given subject molecule. The observed CARS spectrum is proportional to the square of the modulus of the third order susceptibility term, which is the sum of a resonant term, χ_r (related to a nuclear displacement term), and a nonresonant term, χ_{nr} (related to electronic displacement). The temperature and concentration of the resonant species can be determined since the CARS signal at $\omega_{as} = 2\omega_1 - \omega_2$ indicates the Boltzman distribution of that molecule. However, a very thorough knowledge of both the spectroscopic parameters of the species of interest (the contribution through χ_r) and the species composition of the gas phase (contribution through the nonresonant susceptibility) (ref 16) is required for proper modeling.

Extensive iterative fitting procedures are necessary to determine the concentration and temperature of species when the gas composition is not known.

Before this extensive modeling and fitting exercise, only qualitative information can be derived regarding approximate temperatures if some very general approximations are made regarding signal generation (χ_r, χ_{nr}, etc.) as a function of the spatial variation of the resonant species. Difficulties in understanding the distribution of the resonant species and its effect on the intensity and shape of the generated spectra can be minimized by the use of a refinement of the CARS technique called BOXCARS (ref 16). However, the greater level of experimental complexity coupled with the significantly reduced signal intensity characteristic of the BOXCARS' configuration makes the application of the simpler colinear CARS attractive for probing hostile combustion environments (refs 13 and 17) such as the muzzle flash investigated. Therefore, the colinear configuration was selected for these feasibility experiments with the knowledge that no certain temperature or species concentration assignments can be made with any degree of confidence as a result of the spatial averaging over temperature, concentration, and composition gradients.

The CARS measurements are often performed in a closed vessel or on a partly shielded flame to minimize any uncertainties introduced by the surrounding atmosphere. (It is difficult to shield or evacuate the atmosphere from the region around the flash event of a gun.) Therefore, a model species must be selected that is not expected to be present anywhere except within the flash-related flow field. H_2 is well suited to be the target molecule for this application because of its absence from the atmosphere and its anticipated presence in the subject flow field (ref 3). Furthermore, CARS spectroscopic analysis at wavelengths corresponding to H_2 Q-branches is attractive because the Q-branch lines are very narrow and no interference by other species is expected. Moreover, considerable modeling and experimental efforts that are directly applicable have already been extended on this molecule (ref 18).

EXPERIMENTAL

Spectroscopy

CARS spectra were generated using the colinear experimental arrangement shown in figure 1. The frequency output of a Quanta-Ray DCR-1A Nd:YAG laser at 1.06 microns (700 mJ) was doubled to produce the pump beam (ω_1) at 0.532 microns (250 mJ) with a bandwidth of near 1 wave number. The ω_1 is divided with the 50% beam splitter (BS1), leaving about 125 mJ available at this wavelength for probing. The dye laser employed is a Quanta-Ray PDL-1 which incorporates side pumped, flowing cells of an oscillator, pre-amplifier, and amplifier design. The dye laser was operated broadband using Exciton LDS-698 dissolved in ethanol with oscillator and amplifier molar concentrations of 1.5×10^{-3} and 5.8×10^{-4}, respectively. To shift the output towards shorter wavelengths, Exciton DCM was also dissolved in ethanol with oscillator and amplifier concentrations of 1.5×10^{-4} and 1.4×10^{-5}, respectively, and added to the LDS-698 in small amounts while the dye laser output was monitored. At 13% dilution (by volume), the dye laser output (ω_2) was centered at about 6880 Å (14,535 cm^{-1}) with a bandwidth of about 210 cm^{-1} (FWHM) and an intensity of approximately 23 mJ.

The ω_1 and ω_2 beams are made colinear with the aid of a reflecting dichroic mirror at ω_1 (M) and a second dichroic (DC) with R_{max} at ω_1 (5300 Å) and T_{max} at ω_2 (6000 Å). The colinear beams are then focused with a 50-mm focal length lens (L1) and recollimated with an identical lens (L2). The three beams are then separated with a prism (P), and ω_1 and ω_2 are dumped in a beam trap. The CARS signal, ω_3, is then focused and introduced into a fiber optic cable and delivered to a 1/4-m monochromator. The fiber used in these experiments is a fused silica/silica design of 1,000-micron diameter, installed in an armored cable.* The signal emerging from the 10-ft fiber optic cable is recollimated and focused onto the 100-micron entrance slit of the monochromator, equipped with a 1800 line/mm grating. Signal detection is made by a Princeton Applied Research silicon intensified tube (SIT) detector and a controller (PAR model 1216).

Data acquisition was made by both a Nicolet model 4094 and model 2092 digital oscilloscopes acting in sample and hold modes. The broadband detection was of low resolution with the FWHM of the calibration Krypton lines near ω_3 being 8 cm^{-1} wide with a resolution of 3.2 cm^{-1} per channel on the model 2092, equivalent to 0.66 cm^{-1} per channel on the model 4094.

Sample flame measurements were made in a simple H_2 diffusion flame which further aided calibration of the system. Typical unreduced spectra are shown in figure 2 for the diffusion flame; figure 3 for room temperature flowing H_2. No attempt was made to model these colinear spectra to determine temperature during these experiments. However, comparison of the data of figure 2 to the data reported by Vanderhoff and Kotlar (ref 18) shows general Q-branch spacing agreement, as is expected. With this configuration and laser intensities, the CARS signal was of sufficient intensity to be visible to the unaided eye, which greatly simplified alignment of the fiber optic cable and associated optics. As a result, a 0.6 optical density (O.D.) filter was required to sufficiently attenuate the signal before it was used in the monochromator. However, during actual experiments with the gun, this filter was removed after the appropriate adjustments were completed with the H_2 flame in the test position.

MANN Gun

A fully instrumented 7.62-mm MANN gun was modified to accept a special firing mechanism (fig. 4). The gun was activated remotely because the primary laser system operated continuously at 10 Hz and the gun had to be fired relative to this time base to maintain laser beam integrity. The receiver and stand were modified to include the mechanical trigger system comprised of the rope, pulley, and solenoid apparatus. A network of flip-flops was assembled to monitor the pulse train generated by the timing circuits of the laser and to trigger various peripheral devices including the data acquisition and the firing sequence. The laser is monitored by the triggering logic and the PAR model 1216 is synchronized to this time base. Therefore, the video output of the SIT is read after each laser pulse but only recorded by the digital scopes for the laser pulse synchronized with the gun event.

---

* Manufactured by General Fiber Optics, Caldwell, New Jersey.

Because of the variability of the gun's firing (overall delay of 520 ms, jitter of ± 20 ms), the statistical probability of having the 10-ms laser pulse occur within the timeframe of the gun event is very low. Of the hundreds of shots fired, only one yielded fully interpretable spectra. Part of this undesirable overall ignition jitter was caused by the triggering mechanism (fig. 3). However, every gun system has an intrinsic firing delay and associated jitter, although several orders-of-magnitude less than those experienced with the experimental system. Due to the kinematics of the linkages involved, a mechanical triggering system will inevitably experience delay and variability. Therefore, while the delay and jitter experienced were unsuitable for this experiment, they were reasonable for the design of the mechanical system and were subsequently used.

The spectroscopy was verified in the laboratory and details of the triggering approach developed before the equipment was moved to the test area (fig. 5). To minimize the shock loading and the accumulation of soot and dirt on the laser optics, the bulk of the laser hardware was installed in the laser room and a hole drilled in the common wall between the two rooms. Only a minimum number of optical components were located in the immediate area of the gun. These components were mounted on two optical rails installed on independent mounts. The rail holding the pair of lenses and the beam separation, turning prism, were fixed to the same mount that positioned the gun. The second rail, containing the two beam dumps, signal beam conditioning optics, and the fiber optic cable, were installed on a heavy-duty camera tripod. The CARS signal was communicated to the spectrometer located in the adjacent room by means of the fiber optic cable and associated optics.

Alignment of the optics was facilitated with the aid of a simple H_2 diffusion flame placed directly in front of the gun muzzle. With the flame burning and the O.D. filter in position, the alignment of the optics could be optimized based on the intensity of the generated CARS signal. Minor adjustments were made after each firing as the focusing lenses (L1 and L2) were displaced slightly by the shock loading. Generally, alignment was required only on the turning prism (P1). The general experimental procedure was as follows:

1. H_2 flame was positioned and lit
2. CARS signal intensity on the monochromator was checked
3. Optics were adjusted as required to maximize intensity
4. Laser was switched to standby, flame removed, and gun loaded
5. Laser operation was resumed and firing sequence started

RESULTS

Because of experimental limitations and timing difficulties, only two gun-firing experiments yielded examples of H_2 Q-branch spectra. Of these, only one data set included interpretable data resolved temporally relative to the muzzle flash occurrence. However, many observations and conclusions can still be drawn from the limited H_2 data as well as the occurrence and intensity of the nonresonant background.

The overall timing and temporal resolution of the gun-related events is shown in figure 6. Because the breech pressure transducer was not calibrated, it only registered the ignition event in the timing logic circuits. A special microphone, designed to sense only the appearance of the initial blast wave, was situated within 1 foot of the muzzle. Its output, a step change in voltage, is included on the same upper trace as the breech pressure. The lower trace shows the output of a 1P28 phototube fitted with 1.2 O.D. filters and located about 3 feet from the muzzle. The phototube was aimed so that both the muzzle flash and the laser light scattered from the focusing lenses and the other optical surfaces were within its field of view. From the upper trace, the time associated with the emergence of the blast wave from the muzzle was about 1.3 ms measured from the peak recorded breech pressure. The muzzle flash recorded by the phototube occurred at about the same time that the blast wave registered, which was typical. The laser fired about 200 μs before the luminous event was recorded by the phototube.

The unreduced spectrum from the same experiment (fig. 7) clearly shows the presence of H_2 during the muzzle flash sequence. A similar unreduced spectra from another shot made at the same initial timing settings is shown in figure 8 but the exact timing details were not recorded. Comparison of the unreduced spectra of the H_2 diffusion flame (fig. 2) and the H_2 from muzzle flash (figs. 7 and 8) shows similar resonant enhancement in the region around 436 nm. The data suggest that the resonant enhancement of the CARS background was produced during the flash event. Furthermore, from the data in figures 2 and 3, the observed spectral peaks in this region can only be associated with H_2 Q-branch transitions (ref 18). It must be concluded that the shape of the spectra shown in figures 7 and 8 was governed by the Boltzman population distribution of the Q-branch transitions of H_2. In these experiments, the presence of the large nonresonant background was partly due to colinear phase matching and relatively low H_2 concentrations in addition to other contributions.

The unreduced spectra of a different experiment where the laser pulse occurred at 1.3 ms before the appearance of visible flash is shown in figure 9. Only the large background was recorded since H_2 was evidently not present as no resonant enhancement was observed. The laser pulse (fig. 10) occurred about 250 μs past the visible portion of the flash event; the nonresonant background is clearly present but no evidence of resonant enhancement exists. Significantly, the intensity of the nonresonant background is greatly reduced from that shown in figure 9 as only the central, most intense portion of the background was recorded. Two possible explanations are immediately apparent to account for this attenuation:

1. Since the second example (fig. 10) occurred after the visible portion of the muzzle flash event, it is probable that particles and soot were present in the flow field. Examination of spark shadowgraphs (fig. 11) taken during a different, unrelated series of experiments but with the same caliber gun confirmed the nature of the flow field. From these shadowgraphs, a dense, particle- and

soot-laden flow field developed before the projectile emerged from the gun tube. This partially transmitting flow field could easily attenuate the incident ω_1 and ω_2 laser beams, reducing the CARS efficiency.

2. Since the physical interaction of the blast wave with the optical mounts was evolved, it was necessary to realign the gun range optics after each experiment. Although the degree of realignment was not extreme, CARS efficiency was strongly dependent on perfect alignment and any deviation would cause a significant reduction in the resultant signal intensity. Therefore either one or more of these conditions caused the observed signal attenuation during and after the flash event. However, based on previous experiments (refs 1 thorough 3), it was not anticipated that significant concentration of H_2 would be present. The fact that CARS measurements of H_2 may not be practical this late in the flash sequence is of no consequence to the present series of experiments.

CONCLUSIONS

Colinear Coherent Anti-Stokes Raman Scattering (CARS) as a diagnostic technique has been successfully demonstrated on a practical combustion system. The reported experiments verified the feasibility of the concept by applying it to a specific problem: generalized muzzle flash. In addition to the successful completion of the experiment, numerous technical problems were documented which require resolution before a more comprehensive series of experiments is begun. Specifically, the problem areas include:

1. Gun and Event Triggering. The technique used in this series of experiments was based on firing the gun at the laser's internally generated time base and is therefore, unsuitable for high temporal resolution spectroscopy. As the actual experimental window probed in time was not predictable and therefore not deducible in advance, the acquisition of data from this technique was fortuitous. Therefore, the technology to provide a probe beam with documented integrity needs to be developed. This type of approach is currently being investigated.

2. Data Acquisition and Interpretation. Numerous experimental difficulties were responsible for the uncertainty in the wavelength assignments of the reported spectra. Normally, this data acquisition and reduction is accomplished with a specially designed multichannel analyzer. Because of time and equipment limitations, this traditional method was not available. Therefore, the alternate approach was developed and shows good promise for future success, provided the required data manipulation tasks can be assigned and completed by a local minicomputer. The hardware and software are currently being developed to provide this capability.

3. Spatial Uncertainty of Colinear CARS. A significant limitation characteristic of colinear versus other CARS configurations is the uncertainty of the signal generation in space. Because of the large distance over which the probe beams interact, the characteristically large background signal produced is responsible for the relatively large signal which encourages applications in

hostile combustion environments. However, since the CARS signal is produced over a large volume, a high degree of uncertainty is introduced because of the spatial concentration variations of the resonanting species that exist in a complex flow field. Because of this uncertainty, any temperature assignments based on colinear CARS spectra represent an average value corresponding to the resonant species spatial variations. The significance of these measurements cannot be determined until additional experimentation assessing the quantifying this effect is completed.

REFERENCES

1. G. Klingenberg, "Spectroscopic Temperature Measurements During the Interior Ballistic Cycle of a Caliber 20 mm Test Fixture Gun," Fraunhofer-Institut Fur Kurzzeitdynamik, Ernst-Mach-Institut, (EMI-AFB), Weil Am Rhein, June 1983.

2. G. Klingenberg, "Analysis of Gun Muzzle Flash Phenomena," Fourth International Symposium on Ballistics, Monterey, CA, October 1978.

3. G. Klingenberg, et al., "Investigation of Combustion Phenomena Associated with the Flow of Hot Propellant Gases--

   I: Spectroscopic Temperature Measurements Inside the Muzzle Flash of a Rifle," Combustion and Flame, vol 27, 1976, pp 163-176.

   II: Gas Velocity Measurements by Laser-Induced Gas Breakdown," vol 27, 1976, pp 177-187.

   III: Experimental Survey of the Formation and Decay of Muzzle Flow Fields and of Pressure Measurements," vol 29, 1977, pp 289-309.

4. H. Trinks and G. Klingenberg, "Gun Muzzle Blast Field Research: Multiphase Flow Aspects and Chemistry of Muzzle Flash Including Chemical Flash Suppression," Proceedings of the Sixth International Symposium on Ballistics, Orlando, FL, October 1981.

5. E. M. Schmidt and D. D. Sheur, "Optical Measurements of Muzzle Blast," AIAA Journal, vol 13, no. 8, 1975, pp 1086-91.

6. J. I. Erdos and P. D. Del Guidice, "Calculations of Muzzle Blast Flow Fields," AIAA Journal, vol 18, no. 8, 1975, pp 1048-55.

7. E. M. Schmit, E. J. Gion, and K. S. Fansier, "Measurement of and in the Muzzle Blast of a 20-mm Cannon," Fourth International Symposium on Ballistics, Monterey, CA, October 1978.

8. "Engineering Design Handbook, Spectral Characteristics of Muzzle Flash," AMCP 706-225, U.S. Army Materiel Command, July 1967.

9. S. Lederman, R. Cresci, and T. Posillico, "Diagnostics of Gun Barrel Propellants," Final Report No. 83-9, Polytechnic Institute of New York, March 1983.

10. A. C. Eckbreth, J. H. Stuffiebeam, and G. M. Dobbs, "CARS Diagnostics for Practical Combustor Probing," Nineteenth JANNAF Combustion Meeting, Greenbelt, MD, October 1982.

11. K. Aron and L. E. Harris, "CARS Studies of Nitramine LOVA Propellant Combustion," Technical Report ARLCD-TR-83045, ARDC, Dover, NJ, November 1983.

12. K. Kajiyama, et al., "N_2 CARS Thermometry in Diesel Engines," SAE Paper No. 82-1036, Journal of Automotive Engineering, vol 90, no. 12, 1982, p 84.

13. J. A. Shirley, A. C. Eckbreth, and R. J. Hall, "Investigation of the Feasibility of CARS Measurement in Scramjet Combustion," Sixteenth Combustion Meeting, CPIA Publication No. 308, 1979.

14. B. Attai, M. Pealat, and J. P. E. Taran, "CARS Diagnostics of Combustion," Paper No. 80-0282, AIAA Journal, 1980.

15. L. A. Rahn, S. C. Johnson, R. C. Farrow, and P. L. Mattern, Report No. 81-8919, Sandia National Laboratories, Livermore, CA, 1982.

16. R. J. Hall and A. C. Eckbreth, Laser Applications, vol 5, R. K. Erf, Ed, Academic Press, New York, 1982.

17. K. Aron and L. E. Harris, "CARS Measurements on LOVA Nitramine Propellants," 20th JANNAF Combustion Meeting, October 1983.

18. J. A. Vanderhoff and A. J. Kotlar, "Application of CARS to Obtain Temperature in Flame Environments," Technical Report ARBL-TR-02417, Ballistics Research Laboratory, Aberdeen Proving Ground, MD, 1982.

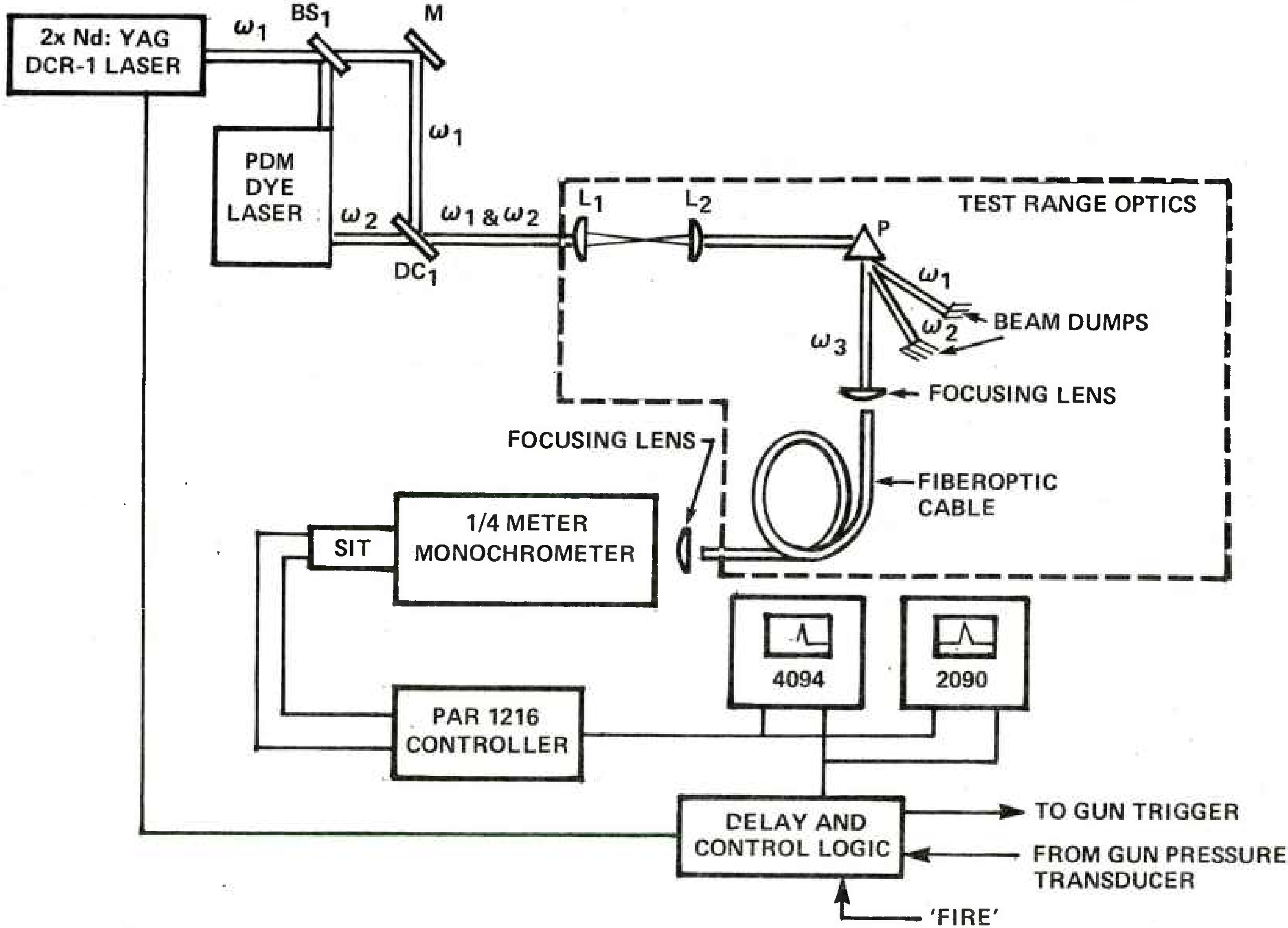

Figure 1. Colinear CARS apparatus [NOTE: BS = 50% beam splitter, M = 100% mirror (ω_1), DC = 100% reflector @ ω_1, 0% @ ω_2, L1 and L2 = focusing lenses, P = prism, and T = beam stops.]

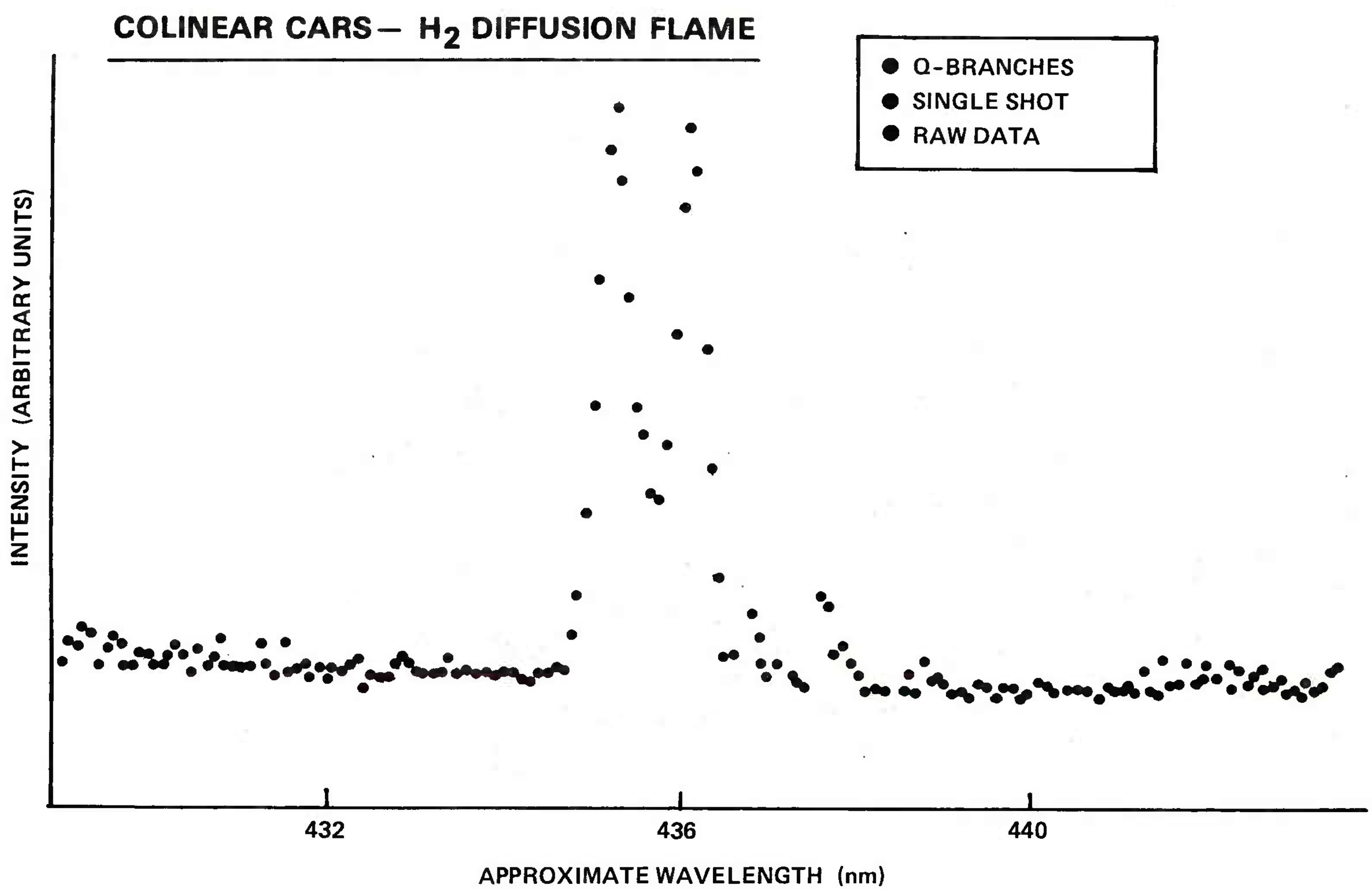

Figure 2. Colinear CARS, H_2 diffusion flame

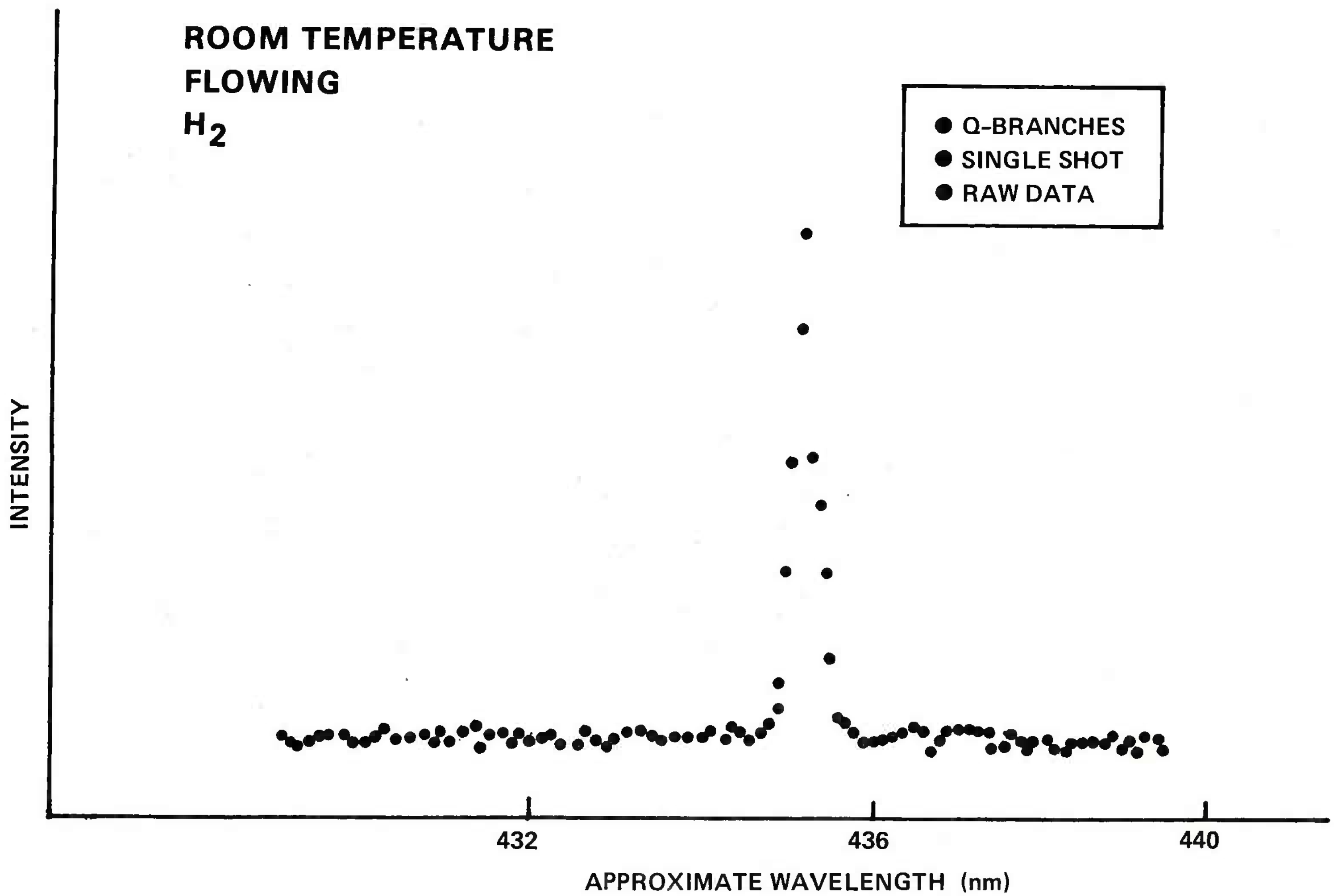

Figure 3. Colinear CARS, room temperature flowing H_2

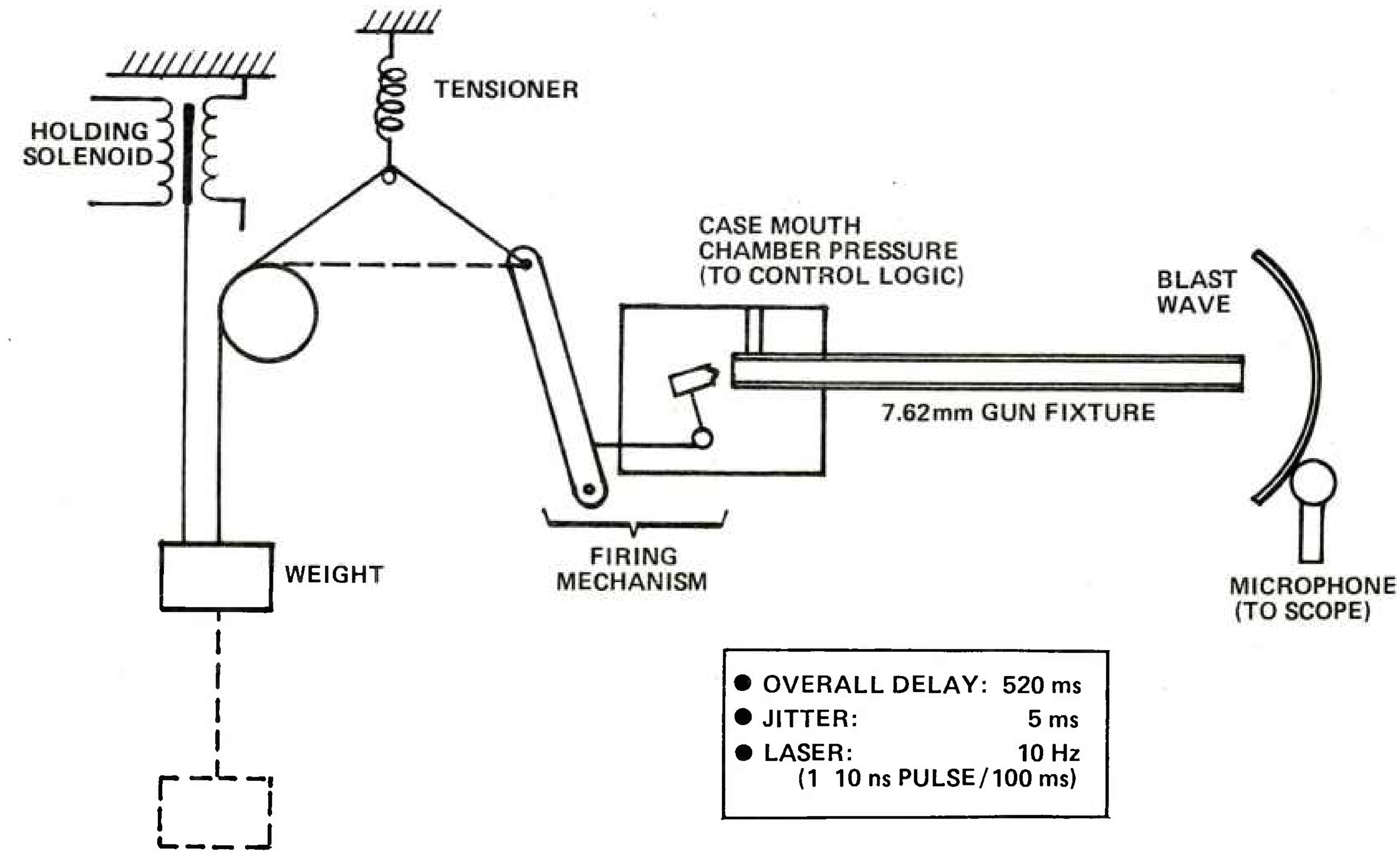

Figure 4. Remote gun trigger

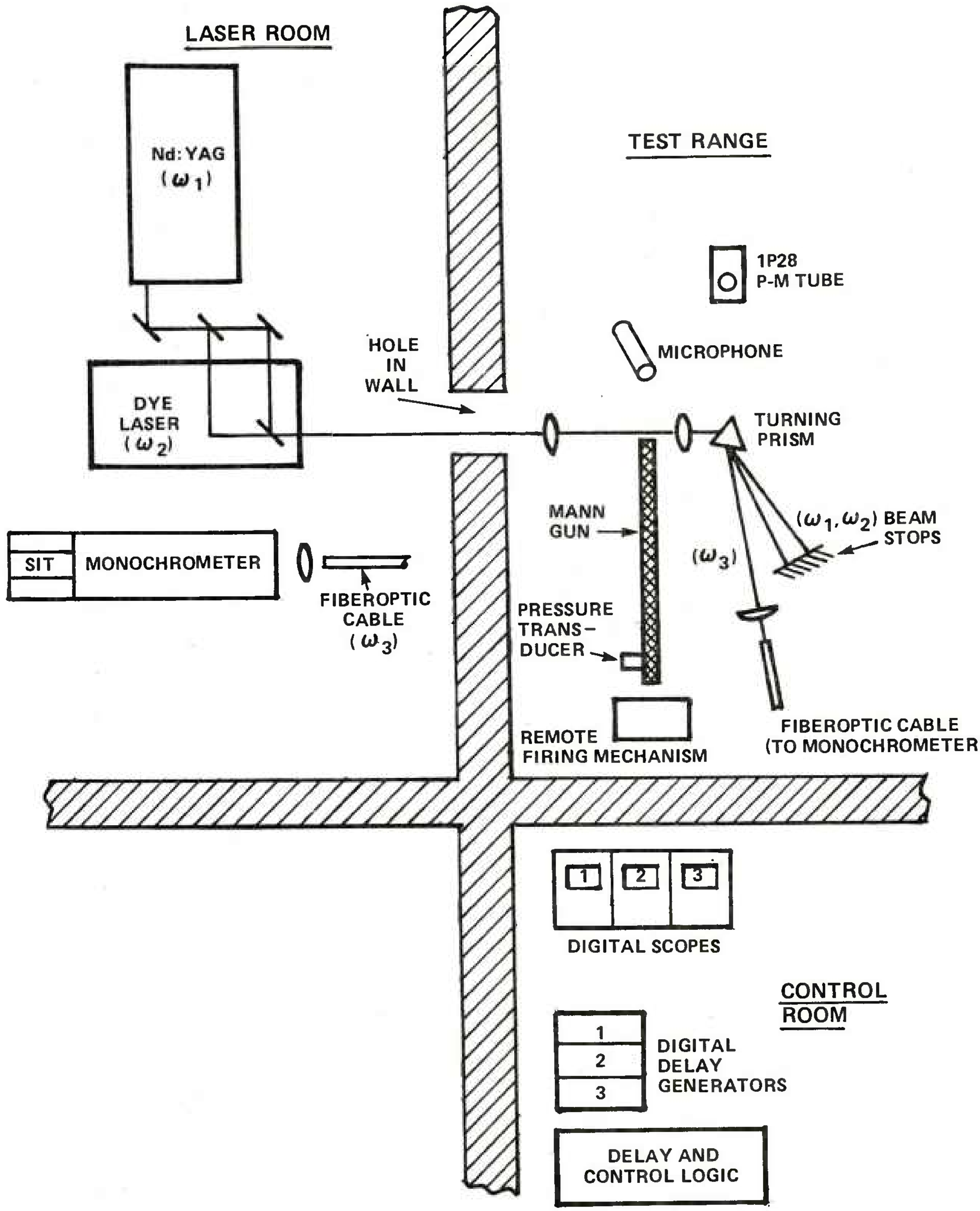

Figure 5. Test area

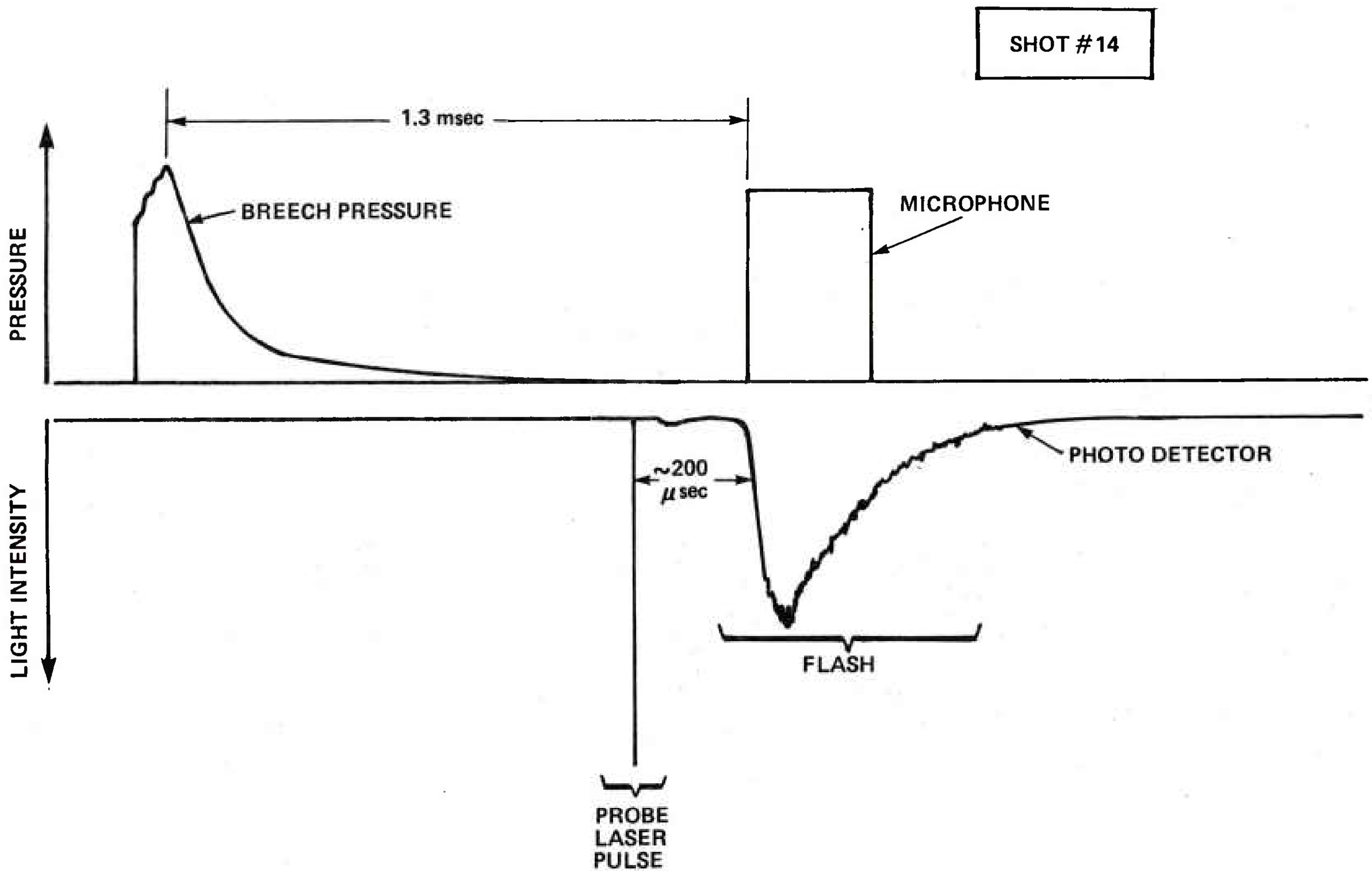

Figure 6. Experimental gun event timing

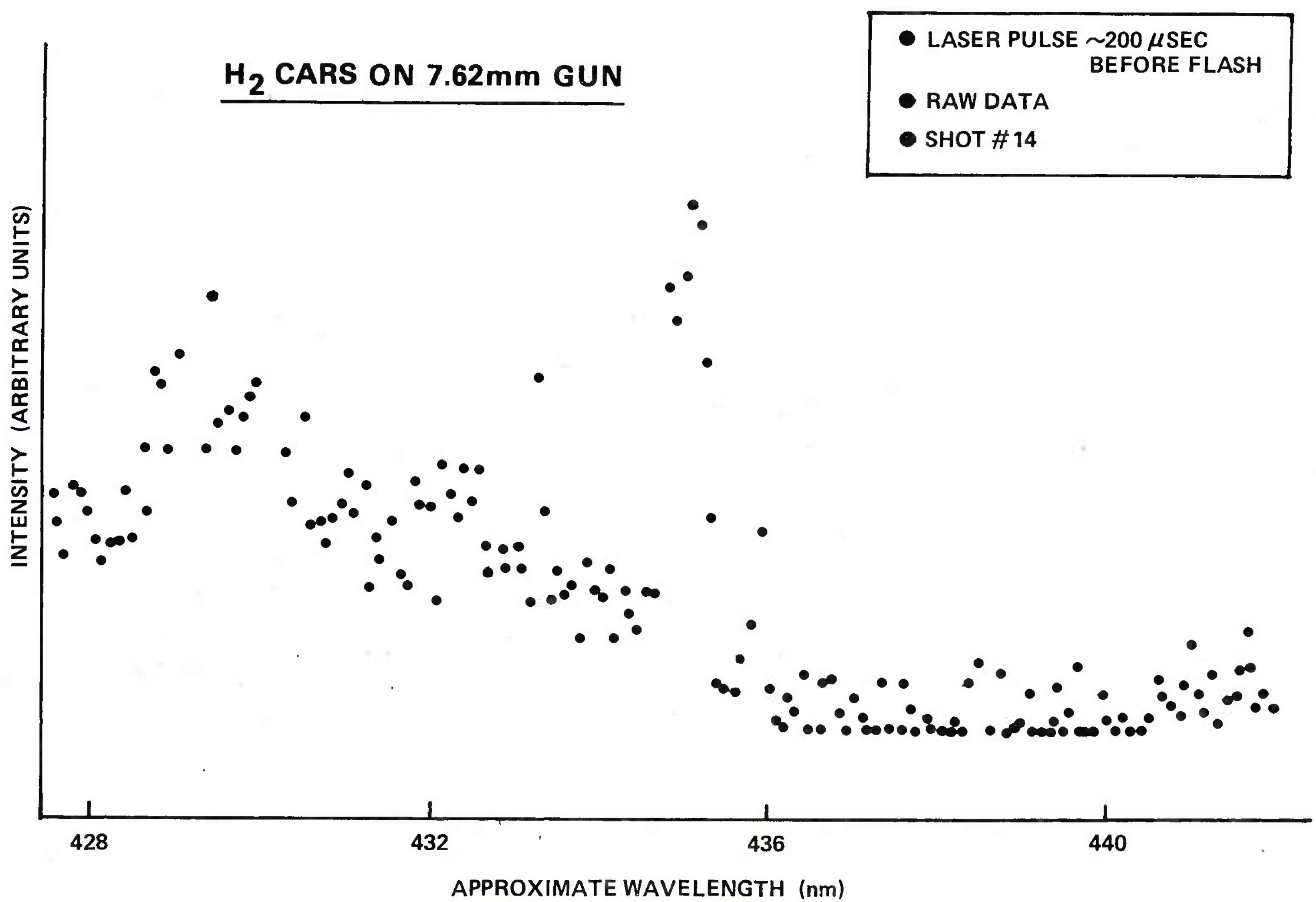

Figure 7. Colinear CARS, H_2 spectra from gun, shot 14

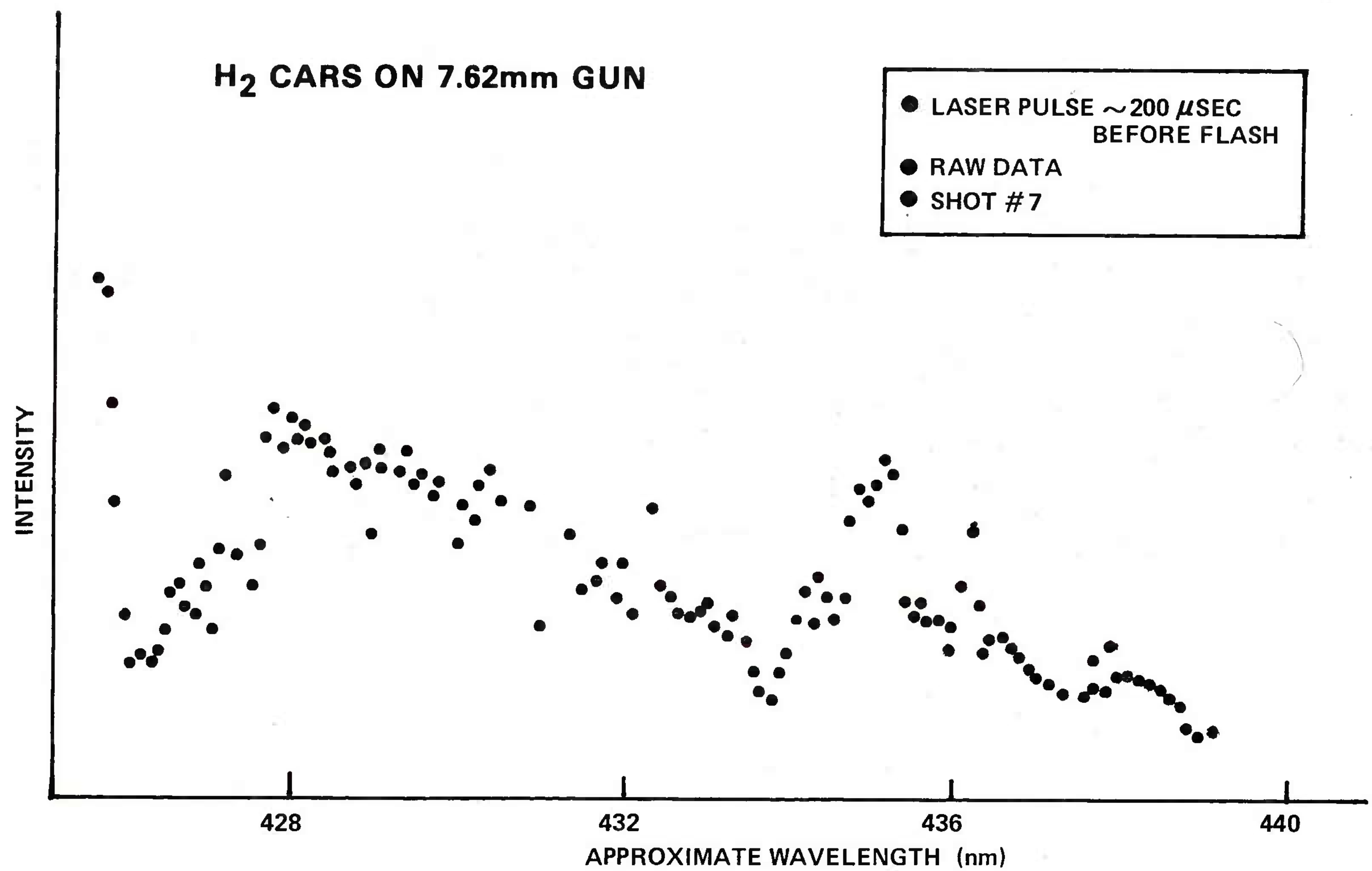

Figure 8. Colinear CARS, H_2 spectra from gun, shot 7

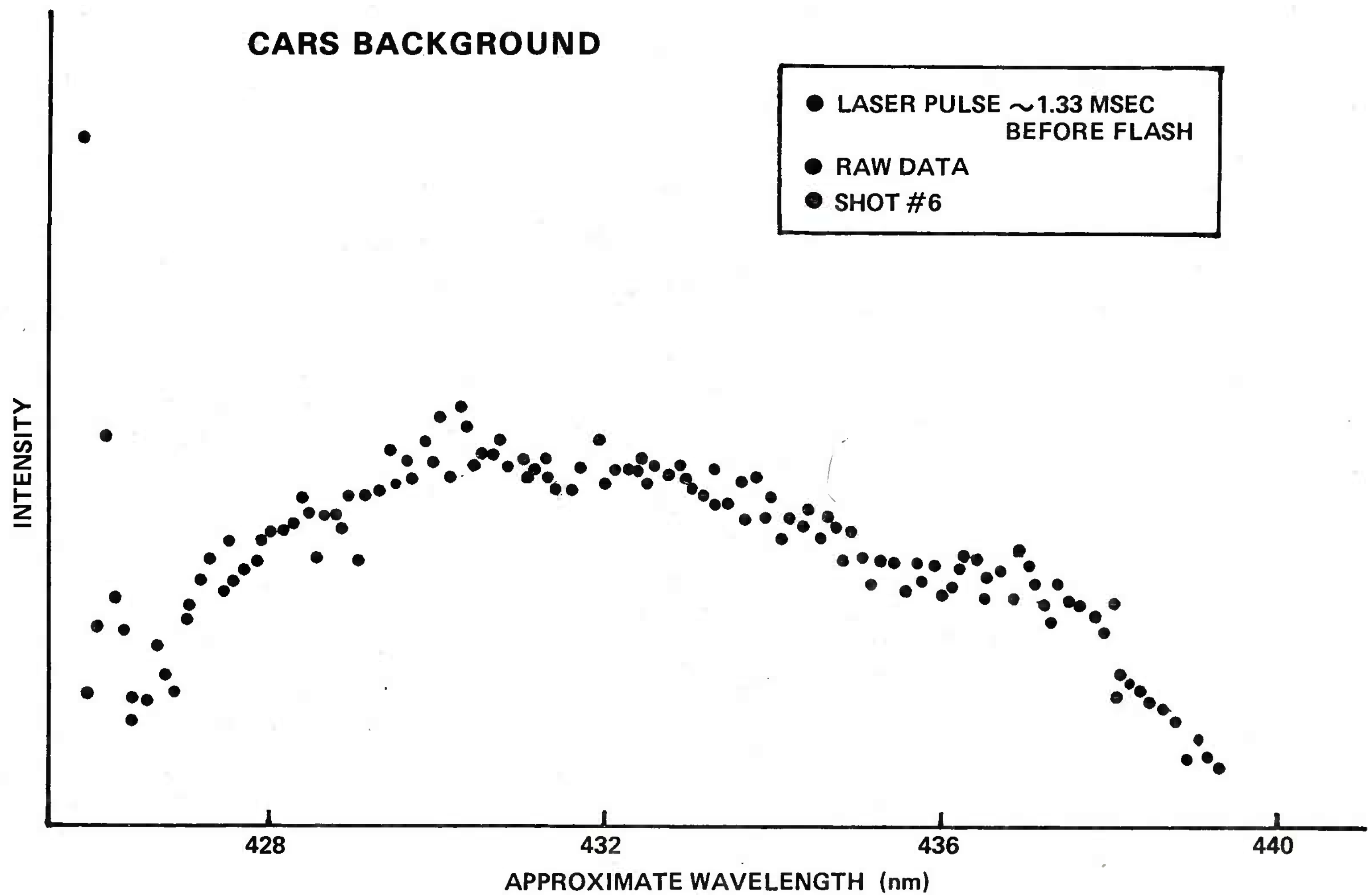

Figure 9. Colinear CARS, background at 1.33 mS before flash

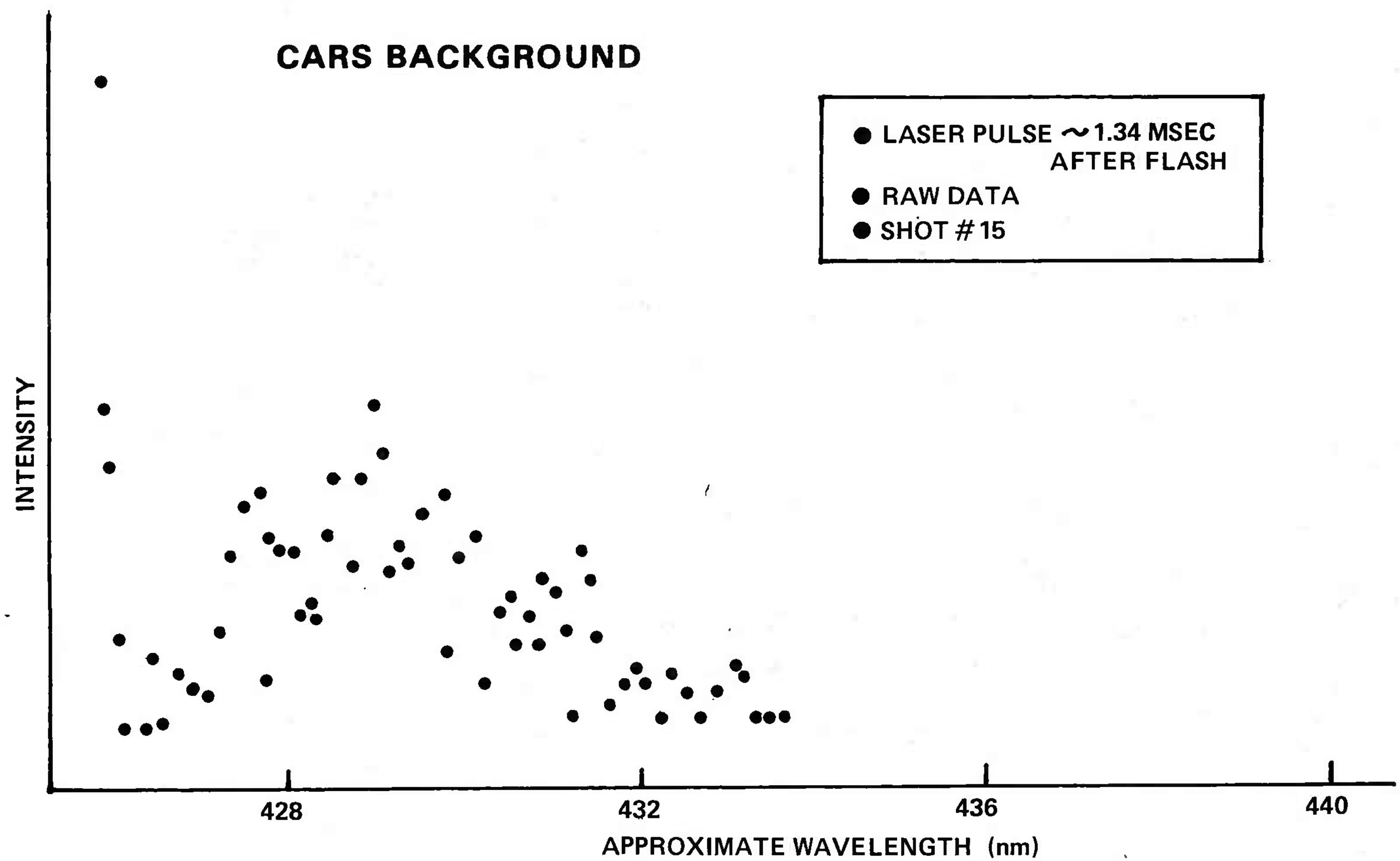

Figure 10. Colinear CARS, background at 1.34 mS after flash

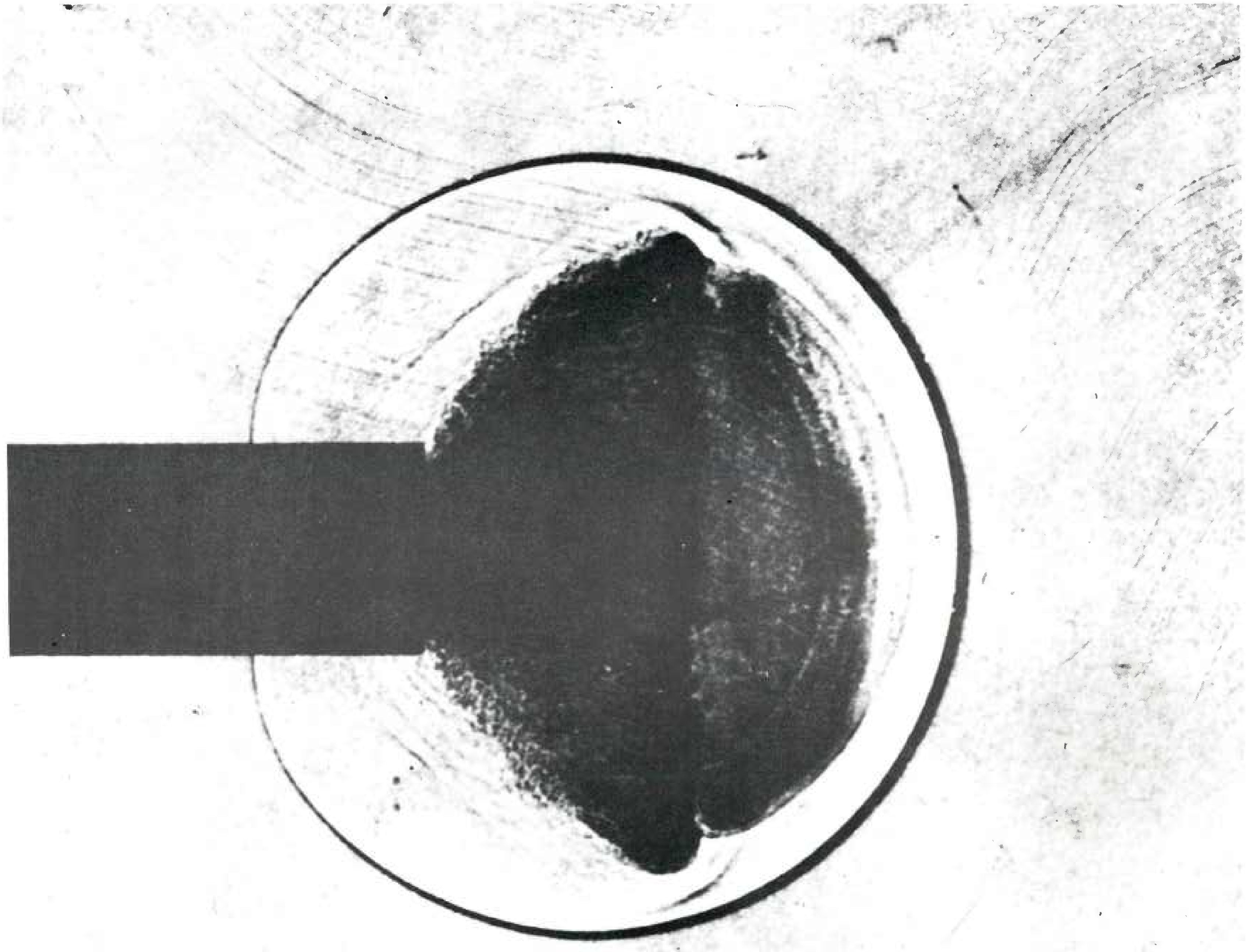

Figure 11. Shadowgraph of muzzle flow field from a 7.62-mm gun

DISTRIBUTION LIST

Commander
Armament Research and Development Center
U.S. Army Armament, Munitions and Chemical Command
ATTN: DRSMC-TSS(D) (5)
DRSMC-TDC(D), D. A. Gyorog
DRSMC-GCL(D)
DRSMC-LC(D), J. Frasier
J. P. Picard
DRSMC-LCA(D), T. Davidson
DRSMC-LCA-G(D), J. Lannon
D. Downs
L. Harris (10)
T. Vladimiroff
A. Beardell
Y. Carignon
J. Fendell
K. Aron
DRSMC-LCE(D), R. Walker
P. Marinkas
C. Capellos
F. Owens
S. Bulusu
F. Gilbert
Dover, NJ 07801

Administrator
Defense Technical Information Center
ATTN: Accessions Division (12)
Cameron Station
Alexandria, VA 22314

Director
U.S. Army Materiel Systems Analysis Activity
ATTN: DRXSY-MP
Aberdeen Proving Ground, MD 21005

Commander
Chemical Research and Development Center
U.S. Army Armament, Munitions and Chemical Command
ATTN: DRSMC-CLJ-L(A)
DRSMC-CLB-PA(A)
APG, Edgewood Area, MD 21010

Director
Ballistics Research Laboratory
Armament Research and Development Center
U.S. Army Armament, Munitions and Chemical Command
ATTN: DRSMC-BLA-S(A)
DRSMC-BLP(A), L. Watermier
A. Barrows
G. Adams
R. Fifer
M. Miller
T. Coffee
J. Heimeryl
C. Nelson
J. Vanderhoff
J. Anderson
Aberdeen Proving Ground, MD 21005

Chief
Benet Weapons Laboratory, LCWSL
Armament Research and Development Center
U.S. Army Armament, Munitions and Chemical Command
ATTN: DRSMC-LCB-TL
Watervliet, NY 12189

Commander
U.S. Army Armament, Munitions and Chemical Command
ATTN: DRSMC-LEP-L(R)
Rock Island, IL 61299

Director
U.S. Army TRADOC Systems
Analysis Activity
ATTN: ATAA-SL
White Sands Missile Range, NM 88002

Director
Defense Advanced Research Projects Agency
ATTN: LTC C. Buck
1400 Wilson Boulevard
Arlington, VA 22209

Commander
U.S. Army Materiel Development and Readiness Command
ATTN: DRCDMD-ST
5001 Eisenhower Avenue
Alexandria, VA 22333

Commander
U.S. Army Watervliet Arsenal
ATTN: SARWV-RD, R. Thierry
Watervliet, NY 12189

Director
U.S. Army Air Mobility Research and Development Laboratory
Ames Research Center
Moffett Field, CA 94035

Commander
U.S. Army Communications Research and Development Command
ATTN: DRDCO-PPA-SA
Fort Monmouth, NJ 07703

Commander
U.S. Army Electronics Research and Development Command
Technical Support Activity
ATTN: DELSD-L
Fort Monmouth, NJ 07703

Commander
U.S. Army Missile Command
ATTN: DRSMI-R
DRSMI-YDL
Redstone Arsenal, AL 35809

Commander
U.S. Army Natick Research and Development Command
ATTN: DRXRE, D. Sieling
Natick, MA 01762

Commander
U.S. Army Tank Automotive Research and Development Command
ATTN: DRDTA-UL
Warren, MI 48090

Commander
U.S. Army White Sands Missile Range
ATTN: STEWS-VT
White Sands Missile Range, NM 88002

Commander
U.S. Army Materials and Mechanics Research Center
ATTN: DRXMR-ATL
Watertown, MA 02172

Commander
U.S. Army Research Office
ATTN: Technical Library
D. Squire
F. Schmiedeshaff
R. Ghirardelli
M. Ciftan
P.O. Box 12211
Research Triangle Park, NC 27706

Office of Naval Research
ATTN: Code 473
G. Neece
800 N. Quincy Street
Arlington, VA 22217

Commander
Naval Sea Systems Command
ATTN: J. W. Murrin, SEA-62R2
National Center
Bldg 2, Room 6E08
Washington, DC 20362

Commander
Naval Surface Weapons Center
ATTN: Library Branch, DX-21
Dahlgren, VA 22448

Commander
Naval Surface Weapons Center
ATTN: Code 240, S. J. Jacobs, J. Sharma
Code 730
Silver Spring, MD 20910

Commander
Naval Underwater Systems Center
Energy Conversion Department
ATTN: Code 5B331, R. S. Lazar
Newport, RI 02840

Commander
Naval Weapons Center
ATTN: R. Derr
C. Thelen
China Lake, CA 93555

Commander
Naval Research Laboratory
ATTN: Code 6180
Washington, DC 20375

Superintendent
Naval Postgraduate School
ATTN: Technical Library
D. Netzer
A. Fuhs
Monterey, CA 93940

Commander
Naval Ordnance Station
ATTN: Charles Dale
Technical Library
Indian Head, MD 20640

AFOSR
ATTN: J. F. Masi
B. T. Wolfson
D. Ball
L. Caveny
Bolling AFB, DC 20332

AFRPL (DYSC)
ATTN: D. George
J. N. Levine
Edwards AFB, CA 93523

National Bureau of Standards
ATTN: J. Hastie
T. Kashiwagi
H. Semerjian
M. Jacox
K. Smyth
J. Stevenson
Washington, DC 20234

Lockheed Palo Alto Research Laboratories
ATTN: Technical Information Center
3521 Hanover Street
Palo Alto, CA 94304

Aerojet Solid Propulsion Co.
ATTN: P. Micheli
Sacramento, CA 95813

Atlantic Research Corporation
ATTN: M. K. King
5390 Cherokee Avenue
Alexandria, VA 22314

AVCO Corporation
AVCO Everett Research Laboratory Division
ATTN: D. Stickler
2385 Revere Beach Parkway
Everett, MA 02149

Calspan Corporation
ATTN: E. B. Fisher
A. P. Trippe
P.O. Box 400
Buffalo, NY 14221

General Electric Company
Armament Department
ATTN: M. J. Bulman
Lakeside Avenue
Burlington, VT 05402

General Electric Company
Flight Propulsion Division
ATTN: Technical Library
Cincinnati, OH 45215

Hercules Incorporated
Alleghany Ballistic Lab
ATTN: R. Miller
Technical Library
Cumberland, MD 21501

Hercules Incorporated
Bacchus Works
ATTN: B. Isom
Magna, UT 84044

IITRI
ATTN: M. J. Klein
10 West 35th Street
Chicago, IL 60615

Olin Corporation
Badger Army Ammunition Plant
ATTN: J. Ramnarace
Baraboo, WI 53913

Olin Corporation
New Haven Plant
ATTN: R. L. Cook
D. W. Riefler
275 Winchester Avenue
New Haven, CT 06504

Paul Gough Associates, Inc.
ATTN: P. S. Gough
P.O. Box 1614
Portsmouth, NH 03801

Physics International Company
2700 Merced Street
Leandro, CA 94577

Pulsepower Systems, Inc.
ATTN: L. C. Elmore
815 American Street
San Carlos, CA 94070

Rockwell International Corp.
Rocketdyne Division
ATTN: C. Obert
J. E. Flanagan
A. Axeworthy
6633 Canoga Avenue
Canoga Park, CA 91304

Rockwell International Corp.
Rocketdyne Division
ATTN: W. Haymes
Technical Library
McGregor, TX 76657

Science Applications, Inc.
ATTN: R. B. Edelman
Combustion Dynamics and Propulsion Division
23146 Cumorah Crest
Woodland Hills, CA 91364

Thiokol Corporation
Elkton Division
ATTN: E. Sutton
Elkton, MD 21921

Thiokol Corporation
Huntsville Division
ATTN: D. Flanigan
R. Glick
Technical Library
Huntsville, AL 35807

Thiokol Corporation
Wasatch Division
ATTN: J. Peterson
Technical Library
P.O. Box 524
Brigham City, UT 84302

TRW Systems Group
ATTN: H. Korman
One Space Park
Redondo Beach, CA 90278

United Technologies
Chemical Systems Division
ATTN: R. Brown
Technical Library
P.O. Box 358
Sunnyvale, CA 94086

Battelle Memorial Institute
ATTN: Technical Library
R. Bartlett
505 King Avenue
Columbus, OH 43201

Brigham Young University
Department of Chemical Engineering
ATTN: M. W. Beckstead
Provo, UT 84601

California Institute of Technology
204 Karmar Lab
Mail Stop 301-46
ATTN: F. E. C. Culick
1201 E. California Street
Pasadena, CA 91125

Georgia Institute of Technology
School of Aerospace Engineering
ATTN: B. T. Zinn
E. Price
W. C. Strahle
Atlanta, GA 30332

Institute of Gas Technology
ATTN: D. Gidaspow
3424 S. State Street
Chicago, IL 60616

Johns Hopkins University/APL
Chemical Propulsion Information Agency
ATTN: T. Christian
Johns Hopkins Road
Laurel, MD 20810

Massachusetts Institute of Technology
Department of Mechanical Engineering
ATTN: T. Toong
Cambridge, MA 02139

Pennsylvania State University
Applied Research Laboratory
ATTN: G. M. Faeth
P.O. Box 30
State College, PA 16801

Pennsylvania State University
Department of Mechanical Engineering
ATTN: K. Kuo
University Park, PA 16801

Pennsylvania State University
Department of Material Sciences
ATTN: H. Palmer
University Park, PA 16801

Princeton Combustion Research Laboratories
ATTN: M. Summerfield
N. Messina
1041 U.S. Highway One North
Princeton, NJ 08540

Princeton University
Forrestal Campus
ATTN: I. Glassman
F. Dryer
Technical Library
P.O. Box 710
Princeton, NJ 08540

Purdue University
School of Mechanical Engineering
ATTN: J. Osborn
S. N. B. Murthy
N. M. Laurendeau
TSPC Chaffee Hall
W. Lafayette, IN 47906

Rutgers State University
Department of Mechanical and Aerospace Engineering
ATTN: S. Temkin
University Heights Campus
New Brunswick, NJ 08903

SRI International
ATTN: Technical Library
D. Crosley
J. Barker
D. Golden
333 Ravenswood Avenue
Menlo Park, CA 94025

Stevens Institute of Technology
W. C. Ermler
Department of Chemistry and Chemical Engineering
Hoboken, NJ 07030

United Technology
ATTN: Alan Ecbreth
Robert Hall
Research Center
East Hartford, CT 06108

Commander
Naval Research Laboratory
Chemistry Division
ATTN: A. Harvey
Washington, DC 20375

General Motors Research Laboratory
ATTN: J. H. Bechtel
Warren, Michigan 48090

System Research Laboratory
ATTN: L. Goss
2600 Indian Ripple Rd
Dayton, Ohio 45440

Exxon Research and Engineering
ATTN: A. Dean
M. Chou
P.O. Box 45
Linden, NJ 07036

Ford Motor Company
Research Staff
ATTN: K. Marko
L. Rimai
Dearborn, Michigan 48120

Sandia Laboratories
Applied Physics Division I
ATTN: L. Rahn
D. Stephenson
Livermore, CA 94550

Rensselaer Polytechnic Institute
Dept. of Chem. Engineering
ATTN: A. Fontijn
Troy, NY 12181

University of California,
San Diego
Ames Department
ATTN: F. Williams
P.O. Box 109
La Jolla, CA 92037

University of California
Dept. of Mechanical Eng.
ATTN: J. W. Daily
Berkeley, CA 94720

University of Dayton
University of Dayton Research Inst.
Dayton, OH 45406

University of Florida
Dept. of Chemistry
ATTN: J. Winefordner
Gainesville, Florida 32601

University of Illinois
Dept. of Mechanical Eng.
ATTN: H. Krier
144 MEB, 1206 W. Green St.
Urbana, IL 61801

University of Minnesota
Dept. of Mechanical Eng.
ATTN: E. Fletcher
Minneapolis, MN 55455

University of California,
Santa Barbara
Quantum Institute
ATTN: K. Schofield
M. Steinberg
Santa Barbara, CA 93106

University of Southern California
Department of Chemistry
ATTN: S. Benson
Los Angeles, CA 90007

Stanford University
Department of Mech. Eng.
ATTN: R. Hanson
Stanford, CA 93106

University of Texas
Department of Chemistry
ATTN: W. Gardiner
H. Schaefer
Austin, TX 78712

University of Utah
Dept. of Chemical Engineering
ATTN: A. Baer
G. Flandro
Salt Lake City, UT 84112

Edward D. Petrow (10)
Geo-Centers, Inc.
Newton Upper Falls, MA 02164